Nanoscale Advances

ROYAL SOCIETY OF CHEMISTRY

PAPER

View Article Online
View Journal | View Issue

Cite this: *Nanoscale Adv.*, 2024, **6**, 4407

Development of a magnified sunlight responsive shape memory bio-composite: effects of titanium nitride (TiN) nanoparticles on a bio-based benzoxazine/epoxy copolymer†

Anandraj Joseph,[a] Ibrahim Lawan,[a] Krittapas Charoensuk,[a] Panuwat Luengrojanakul,[a] Phattarin Mora,[b] Cheol-Hee Ahn[c] and Sarawut Rimdusit *[a]

This study uniquely explored the effects of loading titanium nitride (TiN) nanoparticles in a bio-based benzoxazine/epoxy copolymer on the shape memory performance of the resulting composite using normal and magnified sunlight irradiation stimuli scenarios. Additionally, the effects of loading the TiN nanoparticles in the copolymer on light absorbance capacity, thermal stability, visco-elastic properties, and tensile properties of the composites were analysed. Results reveal that the different loading amounts (1 to 7 wt%) of TiN dispersed well within the copolymer matrix and produced excellent composite samples (TiN-1(wt%), TiN-3(wt%), TiN-5(wt%), and TiN-7(wt%)). Interestingly, the obtained samples were found to exhibit improved light absorbance in the wavelength range of 200–900 nm, giving the samples greater sunlight absorbing capacity. Moreover, the thermal stability of the composites increases with an increase in the loading amount; for instance, the initial degradation temperature increased from 316 °C to 324 °C. Meanwhile, visco-elastic and tensile properties increased and reached the optimum for TiN-5(wt%), where 3.1 GPa and 10.4 MPa were recorded as storage modulus and tensile stress, respectively. Consequent to these improvements in the properties of the composites, the shape memory performance of the composites was positively impacted. For instance, average shape fixity ratio, shape recovery ratio, and recovery time of 95%, 96%, and 38 seconds, respectively, were achieved with TiN-7(wt%), which represents 19%, 17%, and 38% improvements, respectively, compared to when the neat copolymer (TiN-0(wt%)) was used using magnified sunlight irradiation stimulus. Overall, this finding provides the basis for the utilization of magnified sunlight irradiation stimulus to achieve excellent shape memory performance with TiN-filled polymer composites.

Received 30th April 2024
Accepted 29th June 2024

DOI: 10.1039/d4na00360h

rsc.li/nanoscale-advances

Introduction

Shape memory materials (SMMs) are materials that have the unique property of remembering and returning to their original shape under specific conditions.[1] Shape memory polymers (SMPs) are types of SMMs that are made from polymers that have two-phase structures, *viz.* rigid glassy and soft rubbery. The addition of any kind of particles to affect a desired property of the SMP system results in the production of shape memory polymer composites (SMPCs). Generally, SMMs have drawn increasing attention owing to their scientific and technological potential.[2] Potential applications in aerospace, including flexible solar panels, reel-type solar arrays, space-deployable structures and locking mechanisms, have been reported.[3] Other applications of SMMs have also been reported in the biomedical field,[4] self-healing,[5,6] and soft robotics.[7] SMMs are majorly categorized based on the type of external stimuli that trigger their response. Studies related to temperature,[8] magnetic field,[9] electric field,[10] humidity,[11] pH,[12] and light[13] as external stimuli for the shape memory performance of various SMPs/SMPCs have been reported.

Among the various stimuli, light is receiving more attention owing to its advantages in terms of precise remote and wireless control, energy efficiency, and instantaneous on–off properties.[13] Light stimuli could be categorized into four types, *viz.*, ultraviolet light (UV), visible light (VL), infrared light (IR), and sunlight, and each falls within the wavelength range of 10–400 nm, 400–760 nm, 760 nm–1 mm, 10 nm–1 mm, respectively.[13] Many studies involving both thermoplastic and

[a]*Center of Excellence in Polymeric Materials for Medical Practice Devices, Department of Chemical Engineering, Faculty of Engineering, Chulalongkorn University, Bangkok, 10330, Thailand. E-mail: sarawut.r@chula.ac.th*

[b]*Department of Chemical Engineering, Faculty of Engineering, Srinakharinwirot University, Nakhonnayok 26120, Thailand*

[c]*Department of Materials Science and Engineering, Seoul National University, Seoul 08826, Korea*

† Electronic supplementary information (ESI) available. See DOI: https://doi.org/10.1039/d4na00360h

thermosetting polymer SMPCs with UV, VL, and IR as stimuli have been reported, and quite interesting results have been achieved.[13–22] However, sunlight-responsive SMPCs did not receive the attention of the research community in spite of the abundant, energy efficient, cost-effective, and renewable nature of sunlight. Perhaps this is due to the fact that sunlight is a relatively weak source after the long distance it covers to reach the earth's surface and atmospheric filtration.[23]

Therefore, to use the sunlight and stimulate shape memory property, the concept of adding light absorbing fillers for the improvement of sunlight responsive shape memory performance has been applied by two independent research groups,[24,25] to the best of our knowledge. Firstly, Thakur and Karak[24] applied nanohybrid fillers, where TiO_2 and reduced graphene oxide (RGO) were used in amounts ranging from 5 to 10 wt% and 0.5 to 1 wt% as a filler in a hyperbranched polyurethane, respectively, and tested the resulting composite under direct sunlight. Findings revealed that 91.6 to 95.3%, 95.3 to 98.4%, and 1.48 to 7.01 minutes have been achieved as shape fixity ratio, shape recovery ratio, and recovery time, respectively. The addition of the fillers was found to positively impact the thermal stability and mechanical properties of the composite. Secondly, Tian *et al.*[25] developed a composite using TiN and acrylate-terminated polycaprolactone (PCL) and thereafter used an electronic device to simulate sunlight irradiation. The results recorded were ≥93% shape fixity and recovery ratio and 360 seconds recovery time. Thus, it could be seen that the efforts presented so far were only limited to the addition of light absorbing fillers to improve the photothermal efficiency of the composite. Hitherto, efforts towards the magnification of sunlight irradiation to achieve higher shape memory performance have not been reported to the best of our knowledge.

Therefore, this study focused on the development of shape memory bio-composites (SMBs) using bio-based benzoxazine/epoxy copolymer filled with titanium nitride (TiN) nanoparticles and investigation of the resulting composite performance under both normal and magnified sunlight scenarios for the first time. More so, the effects of adding TiN in the composite on the light absorbance capacity, thermal stability, visco-elastic and tensile properties have been studied. TiN was used because of its broadband plasmonic light absorbing capacity and high sunlight absorption efficiency.[26] The bio-based benzoxazine was used due to its molecular design flexibility, easy and cleaner polymerization reaction, near-zero shrinkage after curing[27,28] and the eco-friendly and sustainable reagents used in the synthesis process.[29] The copolymerization of benzoxazine with bio-based epoxy was done to enhance the crosslink density and mechanical properties.[14] The sunlight magnification was achieved using a simple, cost-effective, and zero-energy demanding convex lens (3.5× magnification), and it provides synergistic effects together with the TiN loaded in the composite, as evident by the significantly improved shape memory performance of the composite. The improved shape memory performance achieved using a magnified sunlight stimulation of TiN nanoparticle-filled composites suggests that a novel concept has been established. Therefore, providing useful fundamental information for the efficient utilization of magnified sunlight as a new stimulus for activating SMPCs is the main motivation of this study.

Materials and methods

Materials

Vanillin (99%), furfurylamine (99%), and paraformaldehyde (AR grade) used in the study were obtained from Sigma Aldrich PTE Ltd (Singapore) and Merck Co., Ltd (Darmstadt, Germany), respectively. The epoxidized castor oil (ECO) was provided by Aditya Birla Chemicals Thailand Ltd (Rayong, Thailand), while the titanium nitride (TiN) nanoparticles (99.2%, 20 nm, cubic, 100 g) were purchased from US Research Nanomaterials Inc., Houston, Texas, USA. All the aforementioned materials were used without further treatment.

Development of the TiN filled sunlight responsive shape memory bio-composites

At first, the bio-based benzoxazine/epoxy copolymer was prepared stage-wise by synthesizing the benzoxazine monomer (vanillin furfurylamine (V-fa)) using the solventless method. V-fa was synthesized using vanillin, furfurylamine and paraformaldehyde reagents blended together in a 1 : 1 : 2 molar ratio. The blend was heated at 105 °C for one hour with continuous mixing using a magnetic bar. The obtained transparent clear yellow viscous liquid of V-fa was allowed to settle down at room temperature. Then, the synthesized V-fa and the obtained ECO were blended at a 45 : 55 mass ratio in an aluminium pan and heated at around 130 °C while continuously stirred to obtain the homogenous V-fa/ECO copolymer. Furthermore, the bio-composites were developed by mixing the slightly heated V-fa/ECO copolymer with 1, 3, 5, and 7 wt% concentrations of the TiN differently in an aluminium pan to obtain four different formulations. The composite development process is depicted in Fig. 1.

More so, the four respective homogenous formulations and a neat V-fa/ECO copolymer were poured into an aluminium mold as presented in Fig. 2. The mold containing the five different samples was made to undergo a step-cured process at 150 °C, followed by 160 °C for one hour and then 170 °C followed by 180 °C for two hours in an air circulated oven. Finally, the mold was placed on a hot plate (∼150 °C) and the respective shape memory copolymer and the composites (SMBs) were carefully peeled off the mold and denoted as TiN-0(wt%), TiN-1(wt%), TiN-3(wt%), TiN-5(wt%), and TiN-7(wt%), respectively.

Characterization of the developed bio-composites

Studying the presence and dispersion of the TiN in the matrix. The presence and dispersion of TiN in the matrix were studied using the developed composite samples. The samples were broken to obtain their respective fractured surfaces, and the exposed surfaces were coated with a thin layer of gold using an ion-sputtering device. The gold-coated fractured surfaces were observed and captured using a scanning electron microscope (SEM, JEOL JSM-6510A).

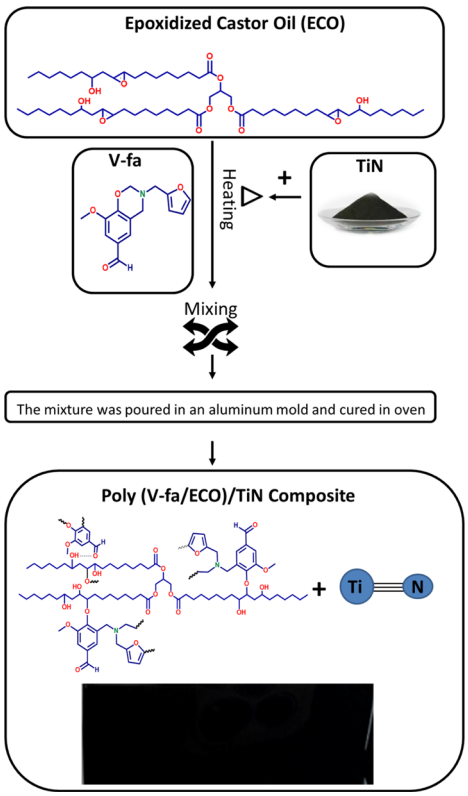

Fig. 1 Development process of the V-fa/ECO/TiN shape memory bio-composite.

Determination of the functional and molecular structure of the bio-composites. The developed samples were characterized for the functional and molecular structure of the cured samples using the Fourier Transform Infrared Spectroscopy (FTIR) (attenuated total reflection (ATR)) within a wavelength range of 4000–400 cm^{-1}.

Determination of light absorbance of the bio-composites. The light absorbance of the neat copolymer and the SMCs was determined using UV-VIS spectrometer equipment (Thermo Scientific Genesys 30) in the wavelength range of 200 to 900 nm.

Determination of thermal stability of the bio-composites. The initial degradation temperature (T_{d5}) and char residue (CR) of the neat copolymer and the SMCs were analysed using a thermogravimetric analyser (TGA) (model TGA 1 STAR^e System from Mettler Toledo) at a heating rate of 20 °C min^{-1} from a temperature of 25 to 800 °C in a nitrogen (N_2) atmosphere. The N_2 was supplied at a steady rate of flow 50 ml min^{-1} throughout the analysis.

Determination of visco-elastic properties of the bio-composites. The storage modulus (E') and glass transition temperature (T_g) of the neat copolymer and the SMCs samples were measured using a dynamic mechanical analyser (DMA) (Mettler Toledo, Switzerland) using the tensile mode. For each of the samples, E' was directly recorded from the dashboard of the DMA, while T_g was obtained as the maximum temperature along the loss tangent (tan δ) curve of the respective samples. Sample dimensions of 20 mm × 5 mm × 0.3 mm, amplitude strain of 5 μm, gauge length of 10 mm, temperature range of −100 to 200 °C, heating rate of 2 °C min^{-1}, and vibration frequency of 1 Hz under an air atmosphere were maintained for each of the samples throughout the tests.

Determination of tensile properties of the bio-composites. The tensile properties of the neat copolymer and the SMBs were evaluated using a universal testing machine (UTM) (Instron 5567, Bangkok, Thailand) through the tension mode. Sample dimensions of 30 mm × 10 mm × 0.3 mm, gauge length of 10 mm, and stretching speed of 5 mm min^{-1} were used for all the samples.

Determination of sunlight responsive shape memory property of the bio-composites. Five specimens each for the neat copolymer and the SMCs samples were cut into a rectangular shape of dimension 55 mm × 15 mm × 0.25 mm. Each of the resized samples was then heated at a temperature of T_g + 20 °C and fitted into a metallic sheet having an angle of 90°. Then, the specimen was allowed to cool to room temperature to achieve a fixed shape shown in Fig. 3. The average and standard deviation for each sample were recorded as fixed angle (θ_f). The prepared fixed samples were then stimulated by normal sunlight and convex lens-magnified sunlight (3.5× magnifier) differently. The experiments were done in Bangkok around April 2024 at noon

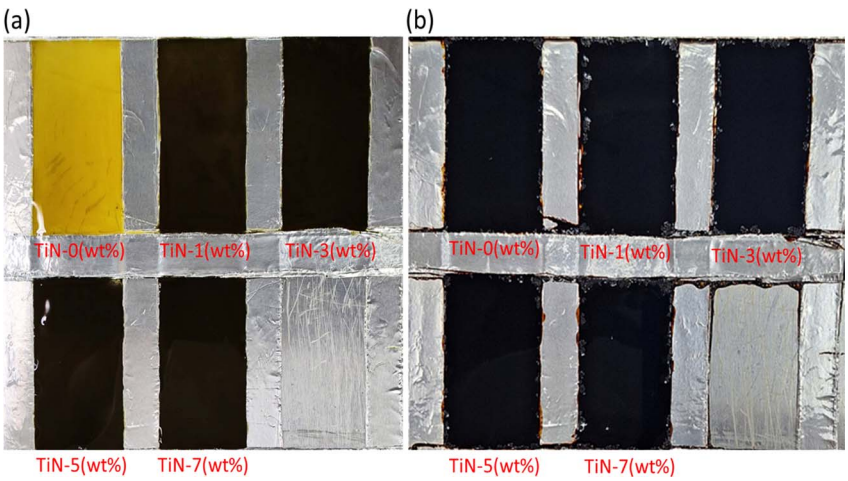

Fig. 2 Neat V-fa and V-fa/ECO/TiN bio-composite formulations poured in aluminium mold (a) before curing and (b) after step curing.

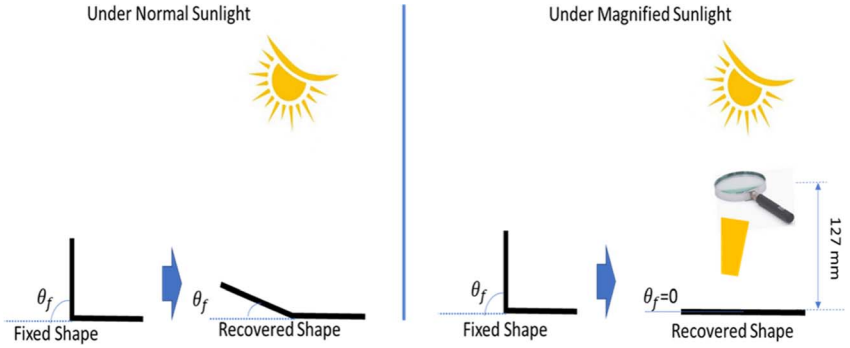

Fig. 3 Shape recovery of the V-fa/ECO/TiN bio-composite actuated by sunlight.

when the temperature ranges between 33 to 34 °C. For the normal sunlight stimulation, the fixed samples were kept on a platform that was totally exposed to normal sunlight and the sample recovery was allowed. On the other hand, the fixed samples were kept on a platform and the magnified sunlight was cast and scanned on the surface of the fixed samples at a focal length of 127 mm until recovery was achieved. For each case, the new θ_f achieved after recovery equals the recovery angle (θ_f). For both scenarios, recovery time (T_r) was recorded using a digital stopwatch, while the shape fixity ratio (R_f) and shape recovery ratio (R_r) were computed using eqn (1) and (2), respectively.

$$R_f = \frac{\theta_f}{90^\circ} \times 100\% \quad (1)$$

$$R_r = \frac{\theta_f - \theta_r}{\theta_f} \times 100\% \quad (2)$$

Results and discussion

Developed TiN filled sunlight responsive shape memory bio-composites

The developed TiN nanoparticle-filled composite samples are depicted in Fig. 2(b), and they were found to be smooth and flexible after removal from the mold.

Presence and dispersion of TiN in the matrix

Fig. 4 depicts the morphologies of the fractured surfaces of the bio-composites. It could be observed that the TiN-0(wt%) (neat V-fa/ECO copolymer) fractured surface shows no presence of the TiN nanoparticles, whereas TiN nanoparticles were obvious on the TiN-1(wt%), TiN-3(wt%), TiN-5(wt%), and TiN-7(wt%) composite fractured surfaces, as expected. The TiN-1(wt%) and TiN-3(wt%) surfaces suggest that the TiN nanoparticles are dispersed in the respective matrices. Similarly, TiN nanoparticle dispersion in the matrices of the TiN-5(wt%) and TiN-7(wt%) composite surfaces could be observed. However, larger agglomeration of TiN nanoparticles was observed in some spots, as circled in Fig. 4(d) and (e). The observed agglomeration could be attributed to the interfacial adhesion between the TiN nanoparticles and V-fa/ECO copolymer. However, the agglomerated particles were covered by the copolymer matrix, thereby maintaining smoothness and a homogenous outlook of the surface morphologies of the composites.

Functional and molecular structure of the bio-composite

Fig. 5 presents the ATR-FTIR absorption spectra of pure TiN, neat copolymer (TiN-0(wt%)), and the SMBs (TiN-1(wt%), TiN-3(wt%), TiN-5(wt%), and TiN-7(wt%)). Fig. 5(a) shows the spectrum of a typical nano-TiN, where an absorption peak at 939 cm^{-1} directly linked to the asymmetric stretching vibration

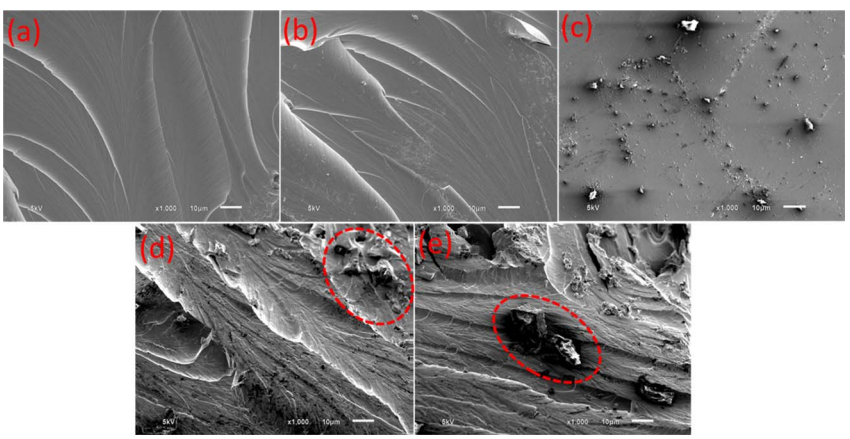

Fig. 4 SEM images of the fractured surfaces of the V-fa/ECO/TiN bio-composite (a) TiN-0(wt%), (b) TiN-1(wt%), (c) TiN-3(wt%), (d) TiN-5(wt%), and (e) TiN-7(wt%).

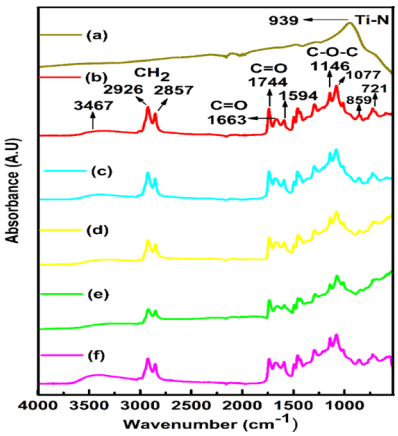

Fig. 5 ATR-FTIR spectra of the TiN and V-fa/ECO/TiN bio-composites (a) TiN, (b) TiN-0(wt%), (c) TiN-1(wt%), (d) TiN-3(wt%), (e) TiN-5(wt%), and (f) TiN-7(wt%).

of TiN groups is exhibited, thereby confirming the presence of titanium directly bonded with nitrogen.[30] The absorption peaks at 3467 cm^{-1}, 2926 cm^{-1} and 2857 cm^{-1}, 1744 cm^{-1} and 1663 cm^{-1}, and 1594 cm^{-1} are assigned to the O–H phenolic hydroxyl group, CH_2 stretching vibration or aliphatic C–H stretching, and C=O stretching, confirming the presence of the carbonyl group of vanillin, and C=O stretching vibration of the furan group (trisubstituted benzene ring) in the V-fa monomer, respectively. The absorption peak at 1146 cm^{-1} correlated to the C–O–C asymmetric ester vibration of ECO, while the absorption peak at 1077 cm^{-1} revealed the presence of the C–O–C stretching mode of ether, which is adjacent to the oxazine ring and the 721 cm^{-1} could be attributed to the C–H out of plane in-phase wagging of the furan moiety. More so, it could be observed that the absorbance peak of C–O–C was slightly modified due to the loading of TiN nanoparticles in the system. For instance, the intensity trends were lowered in the case of Fig. 5(e) and (f) spectra, implying that higher loadings in TiN-5(wt%) and TiN-7(wt%) composites slightly diminish the C–O–C peak.

Light absorbance of the bio-composites

The light absorbance profiles of the neat copolymer and the SMCs are presented in Fig. 6. It could be seen that all the samples exhibited high and stable UV light absorbance, which ranges from 200 to 400 nm. In the case of VL (400 to 760 nm), only the TiN filled SMCs (TiN-1(wt%), TiN-3(wt%), TiN-5(wt%), and TiN-7(wt%)) have exhibited high and stable absorbance throughout the wavelength range. Contrarily, the neat copolymer (TiN-0(wt%)) begins to show a sharp decline in the absorbance from around 718 nm wavelength. Also, a more significant decline in the absorbance of TiN-0(wt%) is exhibited in the IR light range (760 to 900 nm). Therefore, it could be stated that the addition of TiN as a filler in the composite has significantly improved the light absorbance characteristics of the composite, enabling it to have a stable light absorbance from 200 to 900 nm wavelength. This performance of TiN in the composites could be directly linked to the established plasmonic and high light absorbing property of TiN.[25,26]

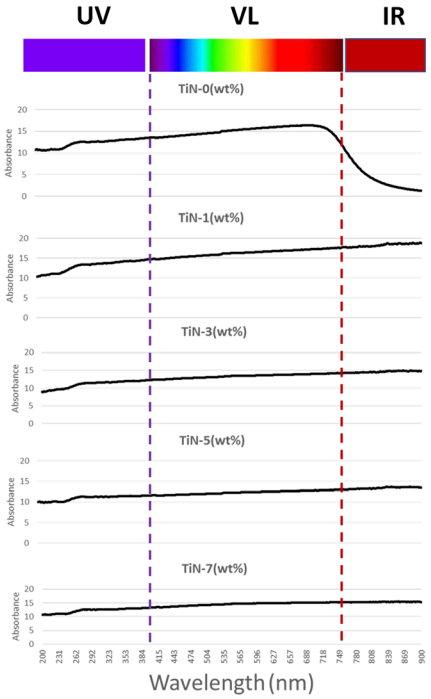

Fig. 6 Light absorbance *versus* wavelength plots of V-fa/ECO/TiN bio-composites.

Thermal stability of the bio-composites

Fig. 7 presents the thermograms of pure TiN, neat copolymer (TiN-0(wt%)), and SMCs (TiN-1(wt%), TiN-3(wt%), and TiN-7(wt%)). An obvious trend showing clear thermal stability of the SMCs could be seen. The thermal stabilities of the samples are in the order TiN-0(wt%) < TiN-1(wt%) < TiN-3(wt%) < TiN-5(wt%) < TiN-7(wt%). This means that the addition of TiN has provided an efficient thermal shield, preventing the composites from thermal degradation. This performance of TiN could be directly attributed to its high thermal stability, depicted in Fig. 7.

Table 1 presents the specific improvements in the thermal stability properties (T_{d5} and CR), where an increase of 2.5% and 32% in T_{d5} and CR, respectively, have been achieved.

Visco-elastic properties of the bio-composites

The values of the visco-elastic properties (E' and T_g) are presented in Table 1. An increase in E' from 1.3 to 2.0 GPa has been recorded, representing a 54% increase. This increase translates to improvements in the rigidity of the composite, which signifies homogenous dispersion, compatibility, and interfacial bonding of TiN in the V-fa/ECO copolymer. A similar trend of results was obtained with regard to the T_g obtained from the tan δ curve of each of the respective samples. The increase ranges from 78 °C for TiN-0(wt%) to 94 °C for TiN-5(wt%), representing ~21% increase. This increase is linked to the

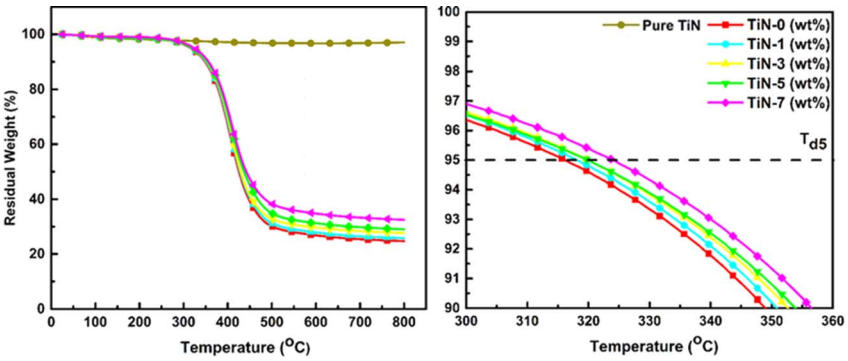

Fig. 7 TGA thermograms and T_{d5} of pure TiN and V-fa/ECO/TiN bio-composites.

Table 1 Thermal stability and visco-elastic properties of V-fa/ECO/TiN bio-composites

	Thermal stability properties		Visco-elastic properties	
Samples	T_{d5} (°C)	CR (%)	E' (GPa)	T_g (°C)
TiN-0(wt%)	316	25	1.3	78
TiN-1(wt%)	318	26	1.8	85
TiN-3(wt%)	319	28	1.9	91
TiN-5(wt%)	320	31	3.1	94
TiN-7(wt%)	324	33	2.0	92

strong interfacial adhesion between the nanofiller and the V-fa/ECO copolymer, which has been established to have an influence on the mobility of the molecular chain and the free volume in the copolymer matrix.[31] However, further loading of TiN on the matrix was seen to cause a decrease in the T_g value to around 92 °C. Perhaps this decrease in the T_g could be due to the aggregation of TiN in the system, which could increase the free volume and molecular chain mobility of the V-fa/ECO copolymer matrix. A similar finding has been reported.[32]

Tensile properties of the bio-composites

Fig. 8 depicts a plot of the tensile stress against the strain of the neat copolymer and the SMBs samples. An increase in the TiN loading from 0 to 5 (wt%) correlates positively with the trend of results recorded for the tensile stress. An increase is observed from 6.5, 6.6, 7.7, and 10.4 MPa, while the strain decreases in the same order, *i.e.*, elongation at break was decreased from 11.2 to 8.7, 5.8, and 4.5 mm mm^{-1}, for TiN-0(wt%), TiN-1(wt%), TiN-3(wt%), and TiN-5(wt%), respectively. The stress and strain values were recorded to be 9.0 MPa and 4.9 mm mm^{-1}, respectively, and did not follow the trend, which could be attributed to the agglomeration of TiN nanoparticles in the TiN-7(wt%) composite.

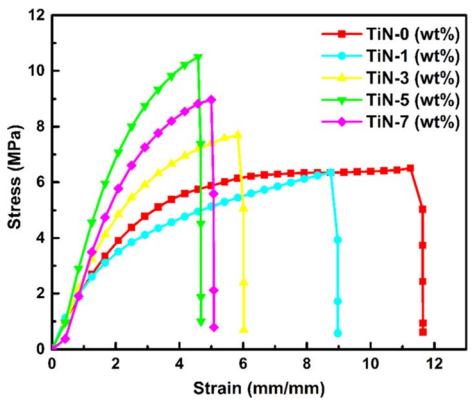

Fig. 8 Tensile stress–strain curves of V-fa/ECO/TiN bio-composites.

Sunlight responsive shape memory property of the bio-composites

The shape fixity ratio (R_f) achieved with the neat V-fa/ECO copolymer and the SMBs is presented in Fig. 9. The increase in R_f with the increase in the TiN nanoparticle filler amount is obvious. The values range from 80 to 95% (Table 2). With reference to the value of R_f for TiN-7(wt%), an improvement of ~19% was achieved. The performance achieved could be attributed to the improvement recorded in the rigidity of the SMBs presented in the previous section. The values of the R_f achieved with the SMBs compare favourably with the R_f reported in previous studies.[14,16] Also, the result of the shape recovery ratio (R_r) with the neat V-fa/ECO copolymer and the SMBs under normal and magnified sunlight is presented in Fig. 9. It could be clearly seen that under normal sunlight, a slight improvement is achieved with the SMBs. For TiN-1(wt%), TiN-3(wt%), TiN-5(wt%), and TiN-7(wt%), values of R_r ranging from 63 to 66% as against the 61% recorded with TiN-0(wt%) (Table 2) are achieved, which translates to about ~8.2% improvement in R_r with TiN-7(wt%). On the other hand, a significant improvement in R_r could be observed with the SMBs under a magnified sunlight scenario. For instance, up to 96% R_r was achieved with TiN-7(wt%) (Table 2), representing ~17% improvement. A similar trend of results is reflected in the recovery time (T_r) parameter. For example, the T_r drops from 130 to 120 seconds to achieve the aforementioned R_r under a normal sunlight scenario, while it took just an average of 38 seconds to achieve almost full recovery of TiN-7(wt%) under the magnified sunlight scenario.

The performance remained almost the same up to the fifth cycle tested, as evidenced by the standard deviations presented

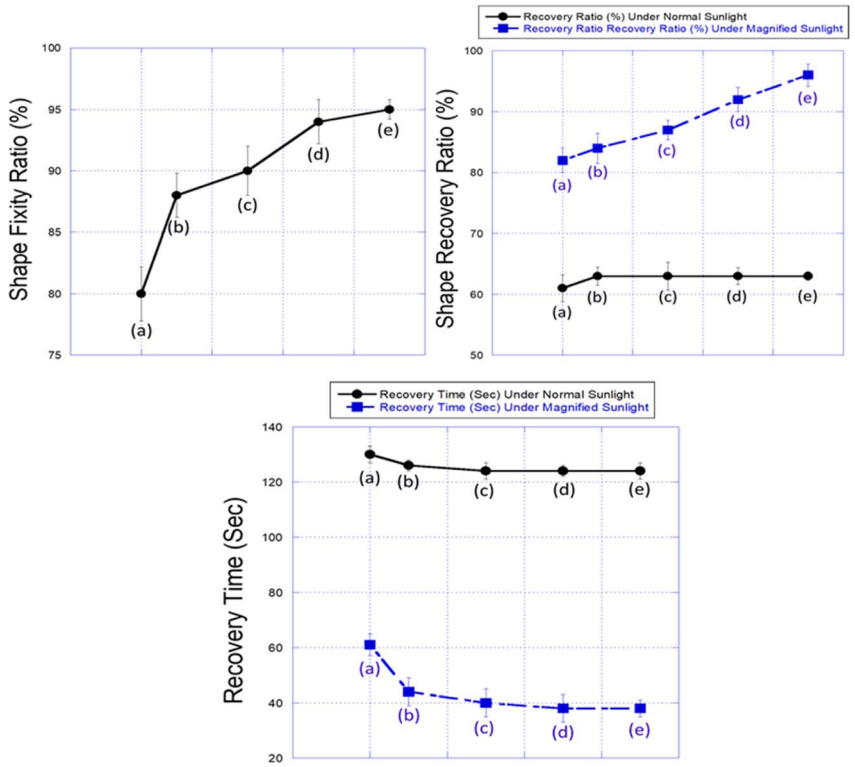

Fig. 9 Shape memory properties of the neat copolymer and V-fa/ECO/TiN bio-composites (a) TiN-0(wt%), (b) TiN-1(wt%), (c) TiN-3(wt%), (d) TiN-5(wt%), and (e) TiN-7(wt%).

(Table 2). Also, the performance of the SMBs suggests that the improvements in light absorbance profile achieved with the addition of TiN in the V-fa/ECO copolymer presented in Fig. 6 have positively impacted the R_r of the SMBs with sunlight stimulation.

Fig. 10 displays a slight increase in the temperature of the SMBs captured at the end of their respective recoveries under normal sunlight scenario, while Fig. 11 also displays a significant increase in the temperature of the SMBs captured at the end of their respective recoveries under magnified sunlight scenario, where it shows an increasing trend with an increase in the amount of TiN nanoparticles. Perhaps this increase in temperatures exhibited by the SMBs could be directly attributed to the improvements in the light absorbance profile achieved with the addition of the TiN nanoparticles, which significantly improved the photothermal efficiency of the SMBs. Thus, it could be summarized that the positive effects of the impact of TiN nanoparticles on the photothermal efficiency of the SMBs have outweighed the increase in the T_g values of the SMBs it has caused, as presented in Table 1. TiN nanoparticles have performed effectively as a filler in the development of the sunlight responsive SMBs, and the performance recorded has outperformed the performance of TiO_2/RGO filled hyperbranched and TiN filled PCL sunlight responsive composites reported by Thakur and Karak[24] and Tian *et al.*,[25] respectively. Additionally, the performance compares favourably with the performance of similar systems reported, such as NIR,[14,16] temperature,[10] and magnetic[14] responsive systems. This suggests that the TiN nanoparticles added in the copolymer in synergy with the magnified sunlight irradiation have significant effects on the

Table 2 Sunlight responsive shape memory properties of V-fa/ECO/TiN bio-composites

			Recovery performance			
			Normal sunlight		Magnified sunlight	
SN	Samples	R_f (%) (heating at T_g + 20 °C)	R_r (%)	T_r (sec)	R_r (%)	T_r (sec)
1	TiN-0(wt%)	80 ± 2.2	61 ± 2.2	130 ± 3	82 ± 2.0	61 ± 4
2	TiN-1(wt%)	88 ± 1.8	63 ± 1.5	126 ± 2	84 ± 2.5	44 ± 5
3	TiN-3(wt%)	90 ± 2.0	63 ± 2.3	124 ± 3	87 ± 1.6	40 ± 5
4	TiN-5(wt%)	94 ± 1.8	65 ± 1.4	120 ± 2	92 ± 2.0	38 ± 5
5	TiN-7(wt%)	95 ± 0.8	66 ± 0.7	120 ± 3	96 ± 1.8	38 ± 3

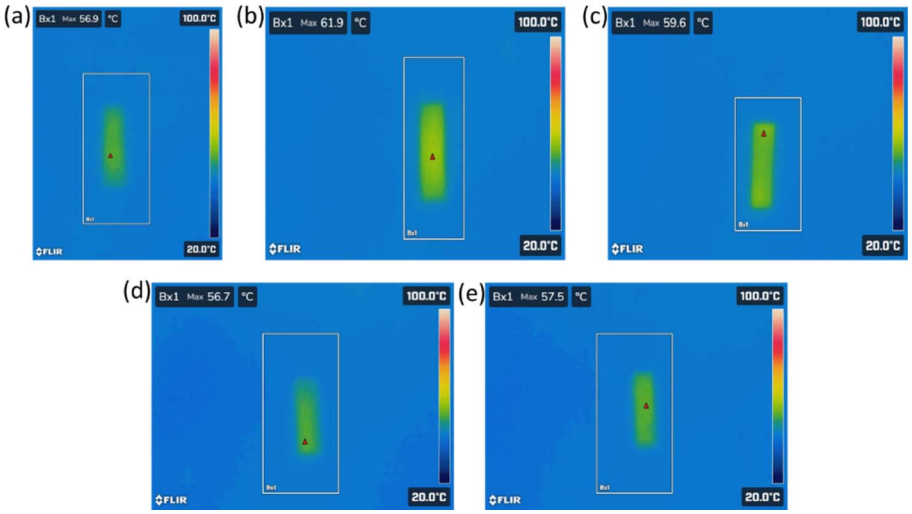

Fig. 10 Temperature images of the V-fa/ECO/TiN bio-composites at the end of recovery under sunlight (a) TiN-0(wt%), (b) TiN-1(wt%), (c) TiN-3(wt%), (d) TiN-5(wt%), and (e) TiN-7(wt%).

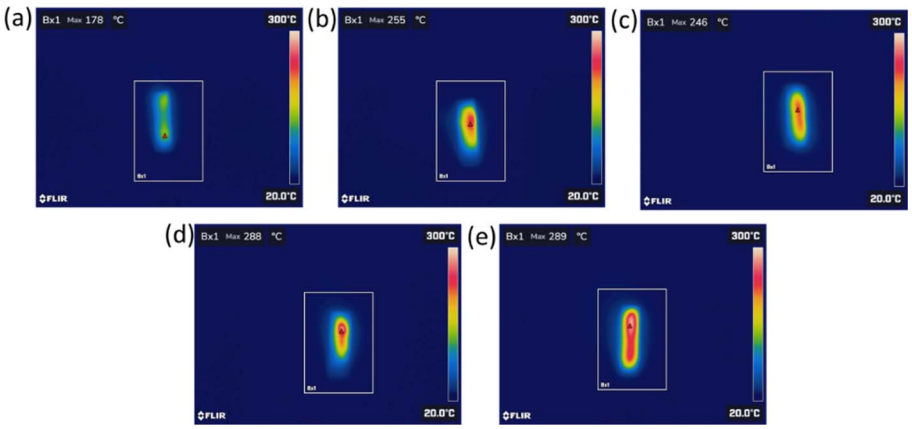

Fig. 11 Temperature images of the V-fa/ECO/TiN bio-composites at the end of recovery under magnified sunlight (a) TiN-0(wt%), (b) TiN-1(wt%), (c) TiN-3(wt%), (d) TiN-5(wt%), and (e) TiN-7(wt%).

shape recovery ratio and time. This performance could be directly attributed to the high optical absorption capacity of the TiN nanoparticles and the concentrated sunlight harvested using the lens.

Conclusion

Based on the results recorded, analysed, and discussed, the following conclusions could be drawn:

(i) The shape memory bio-composites (SMBs) responsive under normal and magnified sunlight have been successfully developed by loading 1, 3, 5, and 7 (wt%) TiN nanoparticles in the V-fa/ECO copolymer.

(ii) Loading TiN nanoparticles in the V-fa/ECO copolymer was found to significantly improve the thermal stability, visco-elastic properties, and tensile properties of the SMBs. Thermal stability increases linearly with an increase in the amount of TiN (1 to 7 (wt%)) in the V-fa/ECO copolymer, whereas visco-elastic and tensile properties reached a maximum with the addition of 5 wt% TiN in the V-fa/ECO copolymer.

(iii). The loading of TiN nanoparticles in the V-fa/ECO copolymer has significantly improved the light absorbance coverage of the composite, making the SMBs have light absorbance up to 900 nm wavelength, thereby making the SMBs have more sunlight absorbance capacity.

(iv) The improved tensile and visco-elastic properties impacted the shape fixity ratio (R_f), where an increase of about 19% was achieved. Meanwhile, the improved sunlight absorbance capacity of the SMBs impacted high photothermal efficiency, which in turn significantly increased the shape recovery ratio (R_r), where about 8.2% and 17% increase was achieved under the normal and magnified sunlight scenarios, respectively. Recovery time (T_r) also drops from 130 to 120 seconds and from 61 to 38 seconds under the normal and magnified sunlight scenarios, respectively.

(v) The significant performance could be attributed to the photonic property of TiN nanoparticles used as the filler in the bio-composite and the concentrated sunlight obtained using the magnification lens.

(vi) Overall, the findings in this study provide broad-based information on how the addition of TiN nanoparticles will improve the photothermal efficiency of composites for shape memory recovery under sunlight. More so, information on how the normal and magnified sunlight stimulates the shape memory recovery of TiN nanoparticle-filled copolymer has been documented for the first time.

Data availability

All relevant data can be made available on request.

Author contributions

Anandraj Joseph: conceptualization, methodology. Ibrahim Lawan: methodology; formal analysis; writing & editing. Krittapas Charoensuk: methodology. Panuwat Luengrojanakul: methodology. Phattarin Mora: conceptualization. Cheol-Hee Ahn: supervision and result validation. Sarawut Rimdusit: supervision, resources, validation, review and editing.

Conflicts of interest

There are no conflicts to declare.

Acknowledgements

This research project is supported by the Second Century Fund (C2F), Chulalongkorn University, National Research Council of Thailand (NRCT) and Chulalongkorn University (N42A660910), and Thailand Science Research and Innovation Fund Chulalongkorn University (No. 6641/2566). The ECO was supported by Aditya Birla Chemical (Thailand) and is gratefully acknowledged.

Notes and references

1 M. Ahmad, D. Singh, Y. Q. Fu, M. Miraftab and J. K. Luo, Stability and deterioration of a shape memory polymer fabric composite under thermomechanical stress, *Polym. Degrad. Stab.*, 2011, **96**, 1470–1477.

2 T. Pretsch, I. Jakob and W. Müller, Hydrolytic degradation and functional stability of a segmented shape memory poly(ester urethane), *Polym. Degrad. Stab.*, 2009, **94**, 61–73.

3 H. Xiao, *et al.*, Shape Memory Polymer Composite Booms with Applications in Reel-Type Solar Arrays, *Chin. J. Mech. Eng.*, 2023, 67.

4 W. Zhao, L. Liu, F. Zhang, J. Leng and Y. Liu, Shape memory polymers and their composites in biomedical applications, *Mater. Sci. Eng., C*, 2019, **97**, 864–883, DOI: **10.1016/j.msec.2018.12.054**.

5 P. C. JE, *et al.*, Manufacturing challenges in self-healing technology for polymer composites — a review, *J. Mater. Res. Technol.*, 2020, **9**, 7370–7379, DOI: **10.1016/j.jmrt.2020.04.082**.

6 F. Orozco, *et al.*, Electroactive Self-Healing Shape Memory Polymer Composites Based on Diels-Alder Chemistry, *ACS Appl. Polym. Mater.*, 2021, **3**, 6147–6156.

7 J. Shin, Y. J. Han, J. H. Lee and M. W. Han, Shape Memory Alloys in Textile Platform: Smart Textile-Composite Actuator and Its Application to Soft Grippers, *Sensors*, 2023, **23**, 1518.

8 Y. Wang, M. Douglas and B. Hazen, Diffusion of public bicycle systems: Investigating influences of users' perceived risk and switching intention, *Transp. Res. A: Policy Pract.*, 2021, **143**, 1–13.

9 Q. Ze, *et al.*, Magnetic Shape Memory Polymers with Integrated Multifunctional Shape Manipulation, *Adv. Mater.*, 2020, **32**, 3184185.

10 M. Y. Razzaq, M. Anhalt, L. Frormann and B. Weidenfeller, Thermal, electrical and magnetic studies of magnetite filled polyurethane shape memory polymers, *Mater. Sci. Eng., A*, 2007, **444**, 227–235.

11 V. Sessini, M. P. Arrieta, A. Fernández-Torres and L. Peponi, Humidity-activated shape memory effect on plasticized starch-based biomaterials, *Carbohydr. Polym.*, 2018, **179**, 93–99.

12 X. J. Han, *et al.*, PH-induced shape-memory polymers, *Macromol. Rapid Commun.*, 2012, **33**, 1055–1060.

13 Y. Wang, Y. Wang, Q. Wei and J. Zhang, Light-responsive shape memory polymer composites, *Eur. Polym. J.*, 2022, **173**, 111314.

14 S. Leungpuangkaew, *et al.*, Magnetic- and light-responsive shape memory polymer nanocomposites from bio-based benzoxazine resin and iron oxide nanoparticles, *Adv. Ind. Eng. Polym. Res.*, 2023, **6**, 215–225.

15 X. Xu, *et al.*, Self-healing thermoplastic polyurethane (TPU)/polycaprolactone (PCL)/multi-wall carbon nanotubes (MWCNTs) blend as shape-memory composites, *Compos. Sci. Technol.*, 2018, **168**, 255–262.

16 W. Jamnongpak, *et al.*, Development of NIR light-responsive shape memory composites based on bio-benzoxazine/bio-urethane copolymers reinforced with graphene, *Nanoscale Adv.*, 2023, **6**, 499–510.

17 L. Amornkitbamrung, *et al.*, Near-infrared light responsive shape memory polymers from bio-based benzoxazine/epoxy copolymers produced without using photothermal filler, *Polymer*, 2020, **209**, 122986.

18 Y. Bai, J. Zhang, D. Wen, P. Gong and X. Chen, A poly (vinyl butyral)/graphene oxide composite with NIR light-induced shape memory effect and solid-state plasticity, *Compos. Sci. Technol.*, 2019, **170**, 101–108.

19 R. Tonndorf, M. Kirsten, R. D. Hund and C. Cherif, Designing UV/VIS/NIR-sensitive shape memory filament yarns, *Text. Res. J.*, 2015, **85**, 1305–1316, DOI: **10.1177/0040517514559578**.

20 L. Yang, *et al.*, Tough self-reporting elastomer with NIR induced shape memory effect, *Giant*, 2021, **8**, 100069.

21 P. Zhang, *et al.*, UV–vis–NIR light-induced bending of shape-memory polyurethane composites doped with azobenzene and upconversion nanoparticles, *Polymer*, 2019, **178**, 121644.
22 M. S. Heo, T. H. Kim, Y. W. Chang and K. S. Jang, Near-infrared light-responsive shape memory polymer fabricated from reactive melt blending of semicrystalline maleated polyolefin elastomer and polyaniline, *Polymers*, 2021, **13**, 3984.
23 H. Kim, *et al.*, RENEWABLE RESOURCES Water Harvesting from Air with Metal-Organic Frameworks Powered by Natural Sunlight, *Science*, 2017, **356**, 430–434, **https://www.science.org**.
24 S. Thakur and N. Karak, Tuning of sunlight-induced self-cleaning and self-healing attributes of an elastomeric nanocomposite by judicious compositional variation of the TiO2-reduced graphene oxide nanohybrid, *J. Mater. Chem. A*, 2015, **3**, 12334–12342.
25 G. Tian, G. Zhu, S. Xu and T. Ren, An Investigation on Sunlight-Induced Shape Memory Behaviours of PCL/TiN Composites Film, *Smart Mater. Struct.*, 2019, **28**, 105006.
26 S. Ishii, K. Uto, E. Niiyama, M. Ebara and T. Nagao, Hybridizing Poly(caprolactone) and Plasmonic Titanium Nitride Nanoparticles for Broadband Photoresponsive Shape Memory Films, *ACS Appl. Mater. Interfaces*, 2016, **8**, 5634–5640.
27 S. Rimdusit, C. Jubsilp and S. Tiptipakorn, *Alloys and Composites of Polybenzoxazines*, Springer Singapore, Singapore, 2013, DOI: **10.1007/978-981-4451-76-5**.
28 K. S. Santhosh Kumar and C. P. Reghunadhan Nair, Polybenzoxazine-new generation phenolics, *Handbook of Thermoset Plastics*, Elsevier Inc., 2014, pp. 45–73, DOI: **10.1016/B978-1-4557-3107-7.00003-8**.
29 M. Uyan and M. S. Celiktas, Evaluation of the bio-based materials utilization in shape memory polymer composites production, *Eur. Polym. J.*, 2023, **195**, 112196.
30 E. Yousefi, M. Ghorbani, A. Dolati, H. Yashiro and M. Outokesh, Preparation of new titanium nitride-carbon nanocomposites in supercritical benzene and their oxygen reduction activity in alkaline medium, *Electrochim. Acta*, 2015, **164**, 114–124.
31 I. Dueramae, A. Pengdam and S. Rimdusit, Highly filled graphite polybenzoxazine composites for an application as bipolar plates in fuel cells, *J. Appl. Polym. Sci.*, 2013, **130**, 3909–3918.
32 S. Srisaard, *et al.*, Effects of graphene nanoplatelets on bio-based shape memory polymers from benzoxazine/epoxy copolymers actuated by near-infrared light, *J. Intell. Mater. Syst. Struct.*, 2022, **33**, 547–557.